

## Helical Luttinger Liquid on a Space-Time Lattice

V. A. Zakharov<sup>1</sup>, J. Tworzydło<sup>2</sup>, C. W. J. Beenakker<sup>1</sup> and M. J. Pacholski<sup>3</sup>

<sup>1</sup>*Instituut-Lorentz, Universiteit Leiden, P.O. Box 9506, 2300 RA Leiden, The Netherlands*

<sup>2</sup>*Faculty of Physics, University of Warsaw, ulica Pasteura 5, 02-093 Warszawa, Poland*

<sup>3</sup>*Max Planck Institute for the Physics of Complex Systems, Nöthnitzer Strasse 38, 01187 Dresden, Germany*

(Received 26 January 2024; revised 22 May 2024; accepted 12 July 2024; published 9 September 2024)

The Luttinger model is a paradigm for the breakdown due to interactions of the Fermi liquid description of one-dimensional massless Dirac fermions. Attempts to discretize the model on a one-dimensional lattice have failed to reproduce the established bosonization results because of the fermion-doubling obstruction: a local and symmetry-preserving discretization of the Hamiltonian introduces a spurious second species of low-energy excitations, while a nonlocal discretization opens a single-particle gap at the Dirac point. Here, we show how to work around this obstruction by discretizing both space and time to obtain a *local* Lagrangian for a helical Luttinger liquid with Hubbard interaction. The approach enables quantum Monte Carlo simulations that preserve the topological protection of an unpaired Dirac cone.

DOI: [10.1103/PhysRevLett.133.116501](https://doi.org/10.1103/PhysRevLett.133.116501)

**Introduction**—A quantum spin Hall insulator [1] supports a one-dimensional (1D) helical edge mode of counterpropagating massless electrons (Dirac fermions, see Fig. 1), with a linear dispersion  $E = \pm \hbar v_F k$ . The crossing at momentum  $k = 0$  (the Dirac point) is protected from gap opening [2] provided that there is only a single species of low-energy excitations and provided that fundamental symmetries (time-reversal symmetry, chiral symmetry) are preserved. This topological protection is broken on a lattice by fermion doubling [3]: any local and symmetry-preserving discretization of the momentum operator  $k = -i\hbar d/dx$  must introduce a spurious second Dirac point [4,5].

Fermion doubling is problematic if one wishes to study interaction effects of 1D massless electrons (a Luttinger liquid [6–9]) by means of a lattice fermion method such as quantum Monte Carlo [10–14]. A way to preserve the time-reversal and chiral symmetries on a lattice is to increase the dimensionality of the system [15,16]. One can simulate a 2D system in a ribbon geometry so that the two fermion species are spatially separated on opposite edges [17–21]. The 2D simulation is computationally more expensive than a fully 1D simulation, but more fundamentally, the presence of states in the bulk may obscure the intrinsically 1D physics of a Luttinger liquid [22]. A 1D simulation using a nonlocal spatial discretization [23] that avoids fermion doubling was studied recently [24] without success: the nonlocality gaps the Dirac point [24,25].

Here, we show that avoiding fermion doubling can be done: a 1D helical Luttinger liquid can be simulated on a lattice if both space *and* time are discretized in a way that preserves the locality of the Lagrangian. The time discretization (in units of  $\tau$ ) pushes the second Dirac point up to energies of order  $\hbar/\tau$ , where it does not affect the low-energy physics, as we demonstrate by comparing quantum

Monte Carlo simulations with results from bosonization [7–9,26].

The lattice fermion approach that we will now describe refers specifically to the massless Dirac fermions that appear in topological insulators. Other approaches exist that exploit the boson-fermion correspondence. One can first bosonize the fermion formulation of the problem [27] and then put it on a lattice [28]. Luttinger liquid physics may also govern the low-energy properties of bosonic systems such as spin chains [29], where fermion doubling does not apply and a lattice formulation poses no difficulties [30,31].

**Locally discretized Lagrangian**—We construct the space-time lattice using the tangent fermion discretization approach [32–37]. We first outline that approach for the noninteracting case in a Lagrangian formulation that is a suitable starting point for the interacting problem.

Consider a 1D free massless fermion field  $\psi_\sigma(x, t)$  with Lagrangian density given by

$$\mathcal{L}_{\text{continuum}} = \sum_{\sigma} \psi_{\sigma}^{\dagger} (i\partial_t + i\sigma v_F \partial_x) \psi_{\sigma}. \quad (1)$$

The spin degree of freedom  $\sigma$ , equal to  $\uparrow\downarrow$  or  $\pm 1$ , distinguishes right-movers from left-movers, both propagating with velocity  $v_F$  along the  $x$  axis. We set  $\hbar = 1$  and

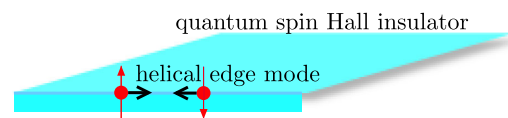


FIG. 1. Helical edge mode consisting of counterpropagating spin-up and spin-down electrons on the 1D boundary of a 2D quantum spin Hall insulator.

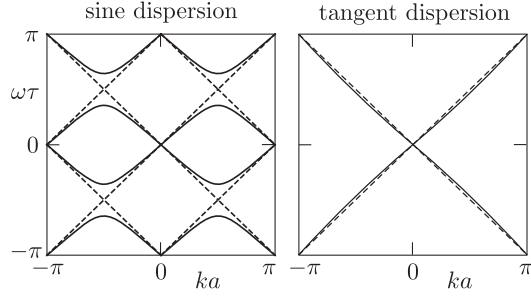


FIG. 2. Dispersion relation of a massless fermion on a 1 + 1-dimensional space-time lattice. The two panels compare the sine and tangent discretization schemes for  $\gamma = v_F\tau/a$  equal to 1 (dashed curves) or 0.9 (solid curves). The sawtooth discretization has the  $\gamma$ -independent dispersion  $\omega = \pm v_F\tau$  in the Brillouin zone  $|\omega\tau|, |ka| < \pi$ . Only the tangent discretization gives a local Lagrangian with a single Dirac point at  $\omega = 0$ .

denote partial derivatives by  $\partial_x, \partial_t$ . The chemical potential is set to zero (the Dirac point, corresponding to a half-filled band).

We discretize space  $x$  and time  $t$  in units of  $a$  and  $\tau$ , respectively. The naive discretization of space replaces  $\partial_x \mapsto (2a)^{-1}(e^{a\partial_x} - e^{-a\partial_x})$ , which amounts to  $\partial_x f(x) \mapsto (2a)^{-1}[f(x+a) - f(x-a)]$ . Similarly,  $\partial_t \mapsto (2\tau)^{-1}(e^{\tau\partial_t} - e^{-\tau\partial_t})$ , producing a Lagrangian with a sine kernel,

$$\mathcal{L}_{\text{sine}} = (a\tau)^{-1} \sum_{\sigma} \psi_{\sigma}^{\dagger} (\sin \hat{\omega}\tau - \sigma\gamma \sin \hat{k}a) \psi_{\sigma}. \quad (2)$$

We defined the frequency and momentum operators  $\hat{\omega} = i\partial_t$  and  $\hat{k} = -i\partial_x$  and denote  $\gamma = v_F\tau/a$ . The discretized  $\psi$ 's are dimensionless.

The naive discretization is a local discretization in the sense that the Lagrangian only couples nearby sites on the space-time lattice. However, it suffers from fermion doubling: the dispersion relation  $\sin \omega\tau = \sigma\gamma \sin ka$  has branches of right-movers and left-movers that intersect at a Dirac point (see Fig. 2, left panel). Kramers' degeneracy protects the crossings at time-reversal invariant points  $\omega\tau, ka = 0$  modulo  $\pi$ . In the Brillouin zone  $|ka|, |\omega\tau| < \pi$  there are four inequivalent Dirac points, two of which are at  $\omega = 0$ : one at  $k = 0$ , the other at  $|k| = \pi$ . Low-energy scattering processes can couple these two Dirac points and open a gap without violating Kramers' degeneracy. To avoid this we need to ensure that there is only a single Dirac point at  $\omega = 0$ .

One way to remove the spurious second species of low-energy excitations goes by the name of SLAC fermions in the particle physics context [23], or Floquet fermions in the context of periodically driven atomic lattices [38,39]. In that approach one truncates the continuum linear dispersion at the Brillouin zone boundaries, and then repeats sawtooth-wise [40] with  $2\pi$ -periodicity,

$$\mathcal{L}_{\text{sawtooth}} = -i(a\tau)^{-1} \sum_{\sigma} \psi_{\sigma}^{\dagger} (\ln e^{i\hat{\omega}\tau} - \sigma\gamma \ln e^{i\hat{k}a}) \psi_{\sigma}. \quad (3)$$

The sawtooth dispersion relation  $\ln e^{i\omega\tau} = \sigma\gamma \ln e^{ika}$  is strictly linear in the Brillouin zone, with a single Dirac point at  $\omega = 0$ ; however the Lagrangian is nonlocal,

$$(\ln e^{i\hat{k}a})f(x) = \sum_{n=1}^{\infty} (-1)^n n^{-1} [f(x-na) - f(x+na)], \quad (4)$$

so distant points on the space-time lattice are coupled.

To obtain a local Lagrangian with a single Dirac point at  $\omega = 0$  we take two steps. First we replace the sine in  $\mathcal{L}_{\text{sine}}$  by a tangent with the same  $2\pi$  periodicity,

$$\mathcal{L}_{\text{tangent}} = \frac{2}{a\tau} \sum_{\sigma} \psi_{\sigma}^{\dagger} [\tan(\hat{\omega}\tau/2) - \sigma\gamma \tan(\hat{k}a/2)] \psi_{\sigma}. \quad (5)$$

The resulting tangent dispersion  $\tan(\omega\tau/2) = \sigma\gamma \tan(ka/2)$  removes the spurious Dirac point (see Fig. 2, right panel), but it creates a nonlocal coupling. The locality is restored by the substitution

$$\psi_{\sigma} = \hat{D}\phi_{\sigma}, \quad \hat{D} = \frac{1}{4}(1 + e^{i\hat{k}a})(1 + e^{i\hat{\omega}\tau}), \quad (6)$$

which produces the Lagrangian

$$\begin{aligned} \mathcal{L}_{\text{tangent}} = & \frac{1}{2}(a\tau)^{-1} \sum_{\sigma} \phi_{\sigma}^{\dagger} [(1 + \cos \hat{k}a) \sin \hat{\omega}\tau \\ & - \sigma\gamma(1 + \cos \hat{\omega}\tau) \sin \hat{k}a] \phi_{\sigma}. \end{aligned} \quad (7)$$

Product terms  $\cos \hat{k}a \times \sin \hat{\omega}\tau$  and  $\cos \hat{\omega}\tau \times \sin \hat{k}a$  couple  $\phi_{\sigma}(x, t)$  to  $\phi_{\sigma}(x \pm a, t \pm \tau)$ , so the coupling is off-diagonal on the space-time lattice but local.

This recovery of a local Lagrangian from a nonlocal Hamiltonian can be understood intuitively [37]: while the tangent discretization of the differential operator is non-local, its functional inverse, which is the trapezoidal integration rule, is local, allowing for a local path integral formulation of the quantum dynamics.

The next step is to introduce the on-site Hubbard interaction (strength  $U$ , repulsive for  $U > 0$ , attractive for  $U < 0$ ) by adding to  $\mathcal{L}_{\text{tangent}}$  the term

$$\mathcal{L}_{\text{Hubbard}} = -(U/a)n_{\uparrow}(x, t)n_{\downarrow}(x, t), \quad n_{\sigma} = :\psi_{\sigma}^{\dagger}\psi_{\sigma}:. \quad (8)$$

The density  $n_{\sigma}$  is normal ordered (Fermi sea expectation value is subtracted). Substitution of Eq. (6) expresses the density  $n_{\sigma}$  at point  $(x, t)$  in terms of the average of the field  $\phi_{\sigma}$  over the four corners of the adjacent space-time unit cell.

This completes the lattice formulation of the Luttinger liquid. We characterize it by the functions

$$\begin{aligned} C_{\sigma}(x) &= \langle \psi_{\sigma}^{\dagger}(x, 0)\psi_{\sigma}(0, 0) \rangle, \quad \Psi = (\psi_{\uparrow}, \psi_{\downarrow}), \\ R_x(x) &= \langle \rho_x(x)\rho_x(0) \rangle, \quad \rho_x(x) = \frac{1}{2}\Psi^{\dagger}(x, 0)\sigma_x\Psi(x, 0). \end{aligned} \quad (9)$$

Here,  $\langle \dots \rangle = Z^{-1} \text{Tr} e^{-\beta H} \dots$  indicates the thermal average at inverse temperature  $\beta = 1/k_B T$  (with  $Z = \text{Tr} e^{-\beta H}$  the partition function). We first focus on the propagator  $C_\sigma$ .

*Discretized Euclidean action*—The propagator can be rewritten as a fermionic path integral [41,42] over anti-commuting fields  $\Psi = \{\Psi_+, \Psi_-\}$  and  $\bar{\Psi} = \{\bar{\Psi}_+, \bar{\Psi}_-\}$ ,

$$C_\sigma(x) = Z^{-1} \int \mathcal{D}\bar{\Psi} \int \mathcal{D}\Psi e^{-\mathcal{S}[\Psi, \bar{\Psi}]} \bar{\Psi}_\sigma(x, 0) \Psi_\sigma(0, 0), \quad (10)$$

with  $\mathcal{S}$  the Euclidean action. For free fermions one has

$$\mathcal{S} = \int_0^\beta dt \int_0^L dx \sum_\sigma \bar{\Psi}_\sigma(x, t) (\partial_t - i\sigma v_F \partial_x) \Psi_\sigma(x, t). \quad (11)$$

The Lagrangian (1) is integrated along the interval  $0 < it < i\beta$  on the imaginary time axis with antiperiodic boundary conditions,  $\Psi_\sigma(x, \beta) = -\Psi_\sigma(x, 0)$ . On the real space axis the integral runs from 0 to  $L$  with periodic boundary conditions,  $\Psi_\sigma(0, t) = \Psi_\sigma(L, t)$ .

The tangent fermion discretization replaces  $i\partial_t \mapsto (2/\tau) \tan(\hat{\omega}\tau/2)$  and  $i\partial_x \mapsto -(2/a) \tan(\hat{k}a/2)$ , resulting in the discretized Euclidean action

$$\begin{aligned} \mathcal{S}_{\text{tangent}} &= 2 \sum_{x,t,\sigma} \bar{\Psi}_\sigma(x, t) (-i \tan(\hat{\omega}\tau/2) \\ &\quad + \gamma\sigma \tan(\hat{k}a/2)) \Psi_\sigma(x, t) \end{aligned} \quad (12a)$$

$$\begin{aligned} &= \frac{1}{2} \sum_{x,t,\sigma} \bar{\Phi}_\sigma(x, t) (-i(1 + \cos \hat{k}a) \sin \hat{\omega}\tau \\ &\quad + \gamma\sigma(1 + \cos \hat{\omega}\tau) \sin \hat{k}a) \Phi_\sigma(x, t). \end{aligned} \quad (12b)$$

In the second equality we substituted the locally coupled fields,  $\Psi = \hat{D}\Phi$ ,  $\bar{\Psi} = \bar{\Phi}\hat{D}^\dagger$ , cf. Eq. (6). The Hubbard interaction is then included by adding to  $\mathcal{S}_{\text{tangent}}$  the action

$$\mathcal{S}_{\text{Hubbard}} = U\tau \sum_{x,t} \bar{\Psi}_+(x, t) \Psi_+(x, t) \bar{\Psi}_-(x, t) \Psi_-(x, t). \quad (13)$$

We choose discretization units  $\tau$ ,  $a$  so that both  $\beta/\tau$  and  $L/a$  are integer. The space-time lattice consists of the points  $it_n = in\tau$ ,  $n = 0, 1, 2, \dots, \beta/\tau - 1$  on the imaginary time axis and  $x_n = na$ ,  $n = 0, 1, 2, \dots, L/a - 1$  on the real space axis. Upon Fourier transformation the sum over  $t_n$  becomes a sum over the Matsubara frequencies  $\omega_n = (2n+1)\pi/\beta$ , while the sum over  $x_n$  becomes a sum over the momenta  $k_n = 2n\pi/L$ . These are odd versus even multiples of the discretization unit to ensure the antiperiodic versus periodic boundary conditions in  $t$  and  $x$ , respectively. In order to avoid the pole in the tangent dispersion we choose  $\beta/\tau$  even and  $L/a$  odd.

*Free-fermion propagator*—Without the interaction term the propagator (10) is given by a Gaussian path integral [41,42], which evaluates to

$$C_\sigma(x) = \frac{\tau}{\beta L} \sum_{k,\omega} \frac{e^{-ikx}}{2i \tan(\omega\tau/2) - 2\gamma\sigma \tan(ka/2)}. \quad (14)$$

A simple closed-form answer follows for the Fourier transform  $C_\sigma(k)$  in the zero-temperature ( $\beta \rightarrow \infty$ ) limit,

$$\begin{aligned} C_\sigma(k) &= \tau \int_{-\pi/\tau}^{\pi/\tau} \frac{d\omega}{2\pi} \frac{1}{2i \tan(\omega\tau/2) - 2\gamma\sigma \tan(ka/2)} \\ &= \frac{-1}{2\text{sign}(\sigma \tan(ka/2)) + 2\gamma\sigma \tan(ka/2)}. \end{aligned} \quad (15)$$

For the sine dispersion we have instead

$$C_\sigma(k) = \frac{-\text{sign}(\sigma \sin ka)}{\sqrt{1 + 4\gamma^2 \sin^2 ka}}, \quad (16)$$

while the sawtooth dispersion gives

$$C_\sigma(k) = -\frac{1}{\pi} \arctan\left(\frac{\pi}{\gamma\sigma ka}\right), \quad |ka| < \pi. \quad (17)$$

Each dispersion has the expected continuum limit [43]  $C_\sigma(k) \rightarrow -\frac{1}{2} \text{sign}(\sigma k)$  for  $|ka| \ll 1$ , up to a factor of 2 for the sine dispersion due to fermion doubling. The difference appears near the boundary  $|ka| = \pi/a$  of the Brillouin zone. As shown in Fig. 3, only the tangent dispersion gives a propagator that is continuous across the Brillouin zone boundary. In real space, the discontinuity shows up as an oscillation of  $C_\sigma(x)$  for separations  $x$  that are even or odd multiples of  $a$ ; see Fig. 4. This is a known artefact of a finite band width [44] that is avoided by tangent fermions: their  $C_\sigma(x)$  is close to the continuum result  $i/2\pi x$  for  $x$  larger than a few lattice spacings.

It is essential that the spatial discretization is accompanied by a discretization of (imaginary) time: if we would

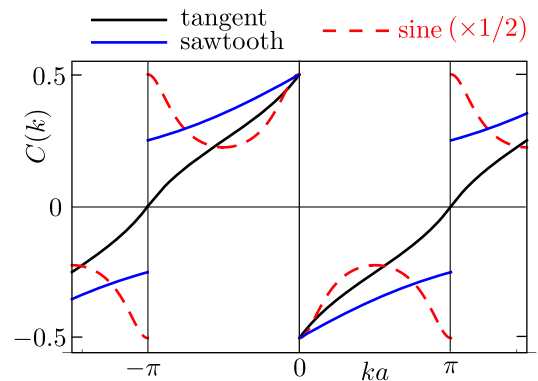


FIG. 3. Free-fermion propagator in momentum space at zero temperature, calculated for three different discretization schemes. The plots follow from Eqs. (15)–(17) for  $\gamma = 1$ ,  $\sigma = +1$ . Only the tangent fermion discretization is continuous at the Brillouin zone boundary  $ka = \pm\pi$ .

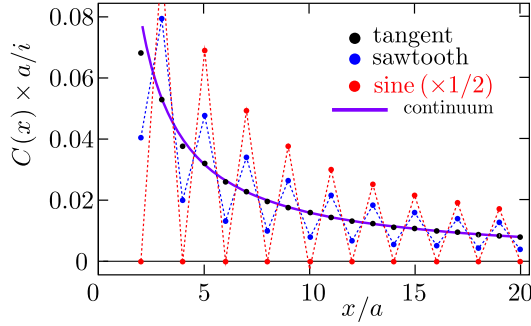


FIG. 4. Same as Fig. 3 but now in real space. The continuum result at zero temperature is  $C(x) = i/2\pi x$  (solid curve), close to the tangent fermion discretization (black dots). The dashed lines are guides to the eye to highlight the oscillatory behavior of the sawtooth and sine discretizations.

only discretize space, taking the limit  $\tau \rightarrow 0$  at fixed  $a$ , then  $\gamma \rightarrow 0$  and the propagator tends to the wrong limit,

$$\lim_{\tau \rightarrow 0} C_\sigma(x) = \frac{1}{2} i\sigma \int_0^{\pi/a} \sin kx dk = \frac{i\sigma \sin^2(\pi x/2a)}{\pi x}, \quad (18)$$

irrespective of how space is discretized. This deficiency of the sawtooth (SLAC) approach was noted in Ref. [24].

*Luttinger liquid correlators*—We now include the Hubbard interaction (13) in the discretized Euclidean action (12), and evaluate the path integral (10) numerically by the quantum Monte Carlo method [45]. In a Luttinger liquid the zero-temperature correlators decay as a power law [8],

$$C_\sigma^2 \propto x^{-K-1/K}, \quad R_x \propto x^{-2K}, \quad (19a)$$

$$K = \sqrt{(1-\kappa)/(1+\kappa)}, \quad \kappa = \frac{Ua}{2\pi v_F} \in (-1, 1). \quad (19b)$$

For repulsive interactions,  $U > 0 \Rightarrow K < 1$ , the transverse spin-density correlator  $R_x$  decays more slowly than the  $1/x^2$  decay expected from a Fermi liquid.

Results for the interaction dependent decay are shown in Fig. 5. The data from the quantum Monte Carlo calculation of  $R_x(x)$  is compared with the predictions from bosonization theory [26]. The power law decay (19) applies to an infinite 1D system. For a more reliable comparison with the numerics we include finite size effects in the bosonization calculations [45].

The finite band width  $1/\tau$  on the lattice requires that the dimensionless interaction strength  $\kappa$  is small compared to unity. As we see in Fig. 5 the agreement with the continuum results (dashed curves) remains quite satisfactory for  $|\kappa|$  up to about 0.4. We stress that this comparison does not involve any adjustable parameter.

*Conclusion*—We have shown that it is possible to faithfully represent an interacting Luttinger liquid on a lattice without compromising the fundamental symmetries of massless fermions. The key step is a space-time discretization of the Lagrangian that is *local* but does not introduce a spurious second species of low-energy excitations. We have tested the validity of this “tangent fermion” approach in the simplest setting where we can compare with the known bosonization results in the continuum.

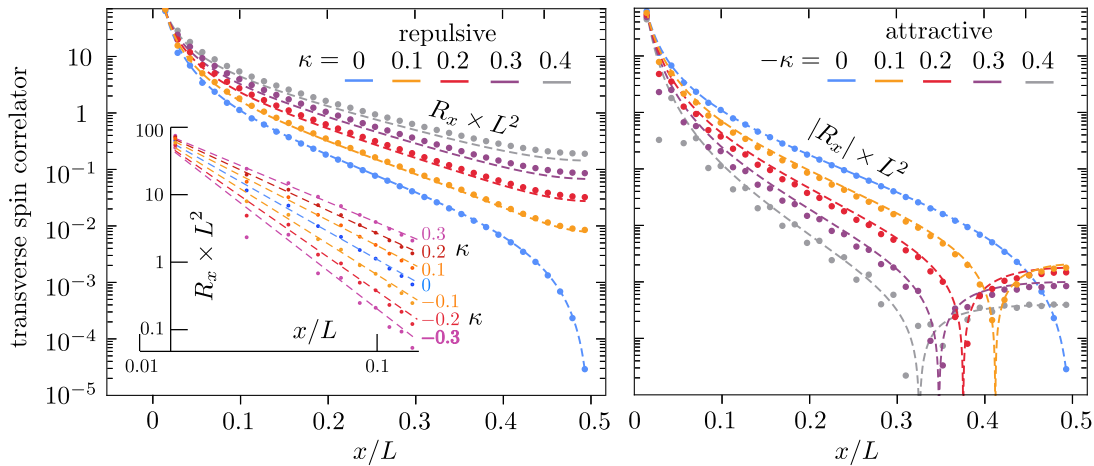


FIG. 5. Main panels: the data points show the quantum Monte Carlo results for the correlator  $R_x(x) = \frac{1}{4} \langle \psi^\dagger(x) \sigma_x \psi(x) \psi^\dagger(0) \sigma_x \psi(0) \rangle$  of the helical Luttinger liquid on the space-time lattice with parameters  $\beta/\tau = 34$ ,  $L/a = 71$ ,  $v_F = a/\tau$ . The different colors refer to different Hubbard interaction strengths  $\kappa = Ua/2\pi v_F$ , repulsive on the left panel and attractive on the right panel. In the latter case the correlator  $R_x$  changes sign; the plot shows the absolute value on a log-linear scale. The  $x$  dependence at  $x$  and  $L-x$  is the same because of the periodic boundary conditions, so only the range  $0 < x < L/2$  is plotted. The numerical data on the lattice is compared with the analytical bosonization theory in the continuum (dashed curves [45]). Note that the lattice calculation slightly overestimates the interaction strength for both the repulsive and attractive cases. The inset in the left panel combines data for both repulsive and attractive interactions on a log-log scale to compare with the power law decay (19) (dashed lines).

We anticipate that tangent fermions can become a powerful tool for the study of topological states of matter, where it is essential to maintain the topological protection of an unpaired Dirac cone. An application to the fermionic Casimir effect was published in Ref. [46]. We have shown that the technique can be applied to quantum Monte Carlo calculations, but we expect it to be more generally applicable to fermionic lattices. Indeed, a second quantized formulation has very recently been used to avoid fermion doubling in the context of tensor networks [47].

*Acknowledgments*—C.B. received funding from the European Research Council (Advanced Grant 832256). J.T. received funding from the National Science Centre, Poland, within the QuantERA II Programme that has received funding from the European Union’s Horizon 2020 research and innovation programme under Grant Agreement No. 101017733, Project Registration Number 2021/03/Y/ST3/00191, acronym TOBITS.

*Data availability*—Our computer codes are provided in a Zenodo repository at [48].

- 
- [1] J. Maciejko, T. L. Hughes, and S.-C. Zhang, The quantum spin Hall effect, *Annu. Rev. Condens. Matter Phys.* **2**, 31 (2011).
- [2] C. L. Kane and E. J. Mele, Quantum spin Hall effect in graphene, *Phys. Rev. Lett.* **95**, 226801 (2005).
- [3] For an overview of methods to avoid fermion doubling in lattice gauge theory see Chapter 4 of David Tong’s lecture notes: <https://www.damtp.cam.ac.uk/user/tong/gaugetheory.html>; Chapter 4 of H. J. Rothe, *Lattice Gauge Theories: An Introduction* (World Scientific, Singapore, 2005).
- [4] H. B. Nielsen and M. Ninomiya, A no-go theorem for regularizing chiral fermions, *Phys. Lett.* **105B**, 219 (1981).
- [5] We are assuming a Hermitian operator. In a non-Hermitian system fermion doubling can be avoided; see M. N. Chernodub, The Nielsen-Ninomiya theorem, PT-invariant non-Hermiticity and single 8-shaped Dirac cone, *J. Phys. A* **50**, 385001 (2017).
- [6] J. M. Luttinger, An exactly soluble model of a many-fermion system, *J. Math. Phys. (N.Y.)* **4**, 1154 (1963).
- [7] F. D. M. Haldane, Luttinger liquid theory of one-dimensional quantum fluids, *J. Phys. C* **14**, 2585 (1981).
- [8] T. Giamarchi, *Quantum Physics in One Dimension* (Oxford University Press, New York, 2003).
- [9] G. Giuliani and G. Vignale, *Quantum Theory of the Electron Liquid* (Cambridge University Press, Cambridge, England, 2008).
- [10] D. J. Scalapino and R. L. Sugar, Method for performing Monte Carlo calculations for systems with fermions, *Phys. Rev. Lett.* **46**, 519 (1981).
- [11] J. E. Hirsch, Discrete Hubbard-Stratonovich transformation for fermion lattice models, *Phys. Rev. B* **28**, 4059 (1983).
- [12] J. E. Hirsch and R. M. Fye, Monte Carlo method for magnetic impurities in metals, *Phys. Rev. Lett.* **56**, 2521 (1986).
- [13] J. Gubernatis, N. Kawashima, and P. Werner, *Quantum Monte Carlo Methods: Algorithms for Lattice Models* (Cambridge University Press, Cambridge, England, 2016).
- [14] F. Becca and S. Sorella, *Quantum Monte Carlo Approaches for Correlated Systems* (Cambridge University Press, Cambridge, England, 2017).
- [15] D. B. Kaplan, Chiral gauge theory at the boundary between topological phases, *Phys. Rev. Lett.* **132**, 141603 (2024).
- [16] D. B. Kaplan and S. Sen, Weyl fermions on a finite lattice, *Phys. Rev. Lett.* **132**, 141604 (2024).
- [17] M. Hohenadler, T. C. Lang, and F. F. Assaad, Correlation effects in quantum spin-Hall insulators: A quantum Monte Carlo study, *Phys. Rev. Lett.* **106**, 100403 (2011).
- [18] Shun-Li Yu, X. C. Xie, and Jian-Xin Li, Mott physics and topological phase transition in correlated Dirac fermions, *Phys. Rev. Lett.* **107**, 010401 (2011).
- [19] Dong Zheng, Guang-Ming Zhang, and Congjun Wu, Particle-hole symmetry and interaction effects in the Kane-Mele-Hubbard model, *Phys. Rev. B* **84**, 205121 (2011).
- [20] Y. Yamaji and M. Imada, Mott physics on helical edges of two-dimensional topological insulators, *Phys. Rev. B* **83**, 205122 (2011).
- [21] In the context of lattice gauge theory, the spatial separation of fermion species is known as the method of domain wall or overlap fermions; see T. Kimura, Domain-wall, overlap, and topological insulators, [arXiv:1511.08286](https://arxiv.org/abs/1511.08286).
- [22] M. Hohenadler and F. F. Assaad, Luttinger liquid physics and spin-flip scattering on helical edges, *Phys. Rev. B* **85**, 081106(R) (2012).
- [23] S. D. Drell, M. Weinstein, and S. Yankielowicz, Strong-coupling field theories. II. Fermions and gauge fields on a lattice, *Phys. Rev. D* **14**, 1627 (1976).
- [24] Z. Wang, F. Assaad, and M. Ulybyshev, Validity of SLAC fermions for the (1+1)-dimensional helical Luttinger liquid, *Phys. Rev. B* **108**, 045105 (2023).
- [25] Yuan Da Liao, Xiao Yan Xu, Zi Yang Meng, and Yang Qi, Caution on Gross-Neveu criticality with a single Dirac cone: Violation of locality and its consequence of unexpected finite-temperature transition, *Phys. Rev. B* **108**, 195112 (2023).
- [26] J. von Delft and H. Schoeller, Bosonization for beginners—re-fermionization for experts, *Ann. Phys. (Berlin)* **510**, 225 (1998).
- [27] L. Alvarez-Gaumé, G. Moore, P. Nelson, C. Vafa, and J. B. Bost, Bosonization in arbitrary genus, *Phys. Lett. B* **178**, 41 (1986).
- [28] E. Berkowitz, A. Cherman, and T. Jacobson, Exact lattice chiral symmetry in 2d gauge theory, [arXiv:2310.17539](https://arxiv.org/abs/2310.17539).
- [29] F. D. M. Haldane, Demonstration of the “Luttinger liquid” character of Bethe-Ansatz-soluble models of 1-D quantum fluids, *Phys. Lett.* **81A**, 153 (1981).
- [30] F. C. Alcaraz and Y. Hatsugai, String correlation functions in the anisotropic spin-1 Heisenberg chain, *Phys. Rev. B* **46**, 13914 (1992).
- [31] A. Urichuk, J. Sirker, and A. Klümper, Analytical results for the low-temperature Drude weight of the XXZ spin chain, *Phys. Rev. B* **103**, 245108 (2021).
- [32] R. Stacey, Eliminating lattice fermion doubling, *Phys. Rev. D* **26**, 468 (1982).

- [33] C. M. Bender, K. A. Milton, and D. H. Sharp, Consistent formulation of fermions on a Minkowski lattice, *Phys. Rev. Lett.* **51**, 1815 (1983).
- [34] J. Tworzydło, C. W. Groth, and C. W. J. Beenakker, Finite difference method for transport properties of massless Dirac fermions, *Phys. Rev. B* **78**, 235438 (2008).
- [35] M. J. Pacholski, G. Lemut, J. Tworzydło, and C. W. J. Beenakker, Generalized eigenproblem without fermion doubling for Dirac fermions on a lattice, *SciPost Phys.* **11**, 105 (2021).
- [36] A. Donís Vela, M. J. Pacholski, G. Lemut, J. Tworzydło, and C. W. J. Beenakker, Massless Dirac fermions on a space-time lattice with a topologically protected Dirac cone, *Ann. Phys. (Berlin)* **534**, 2200206 (2022).
- [37] C. W. J. Beenakker, A. Donís Vela, G. Lemut, M. J. Pacholski, and J. Tworzydło, Tangent fermions: Dirac or Majorana fermions on a lattice without fermion doubling, *Ann. Phys. (Berlin)* **535**, 2300081 (2023).
- [38] J.-C. Budich, Ying Hu, and P. Zoller, Helical Floquet channels in 1D lattices, *Phys. Rev. Lett.* **118**, 105302 (2017).
- [39] Xiao-Qi Sun, Meng Xiao, T. Bzdušek, Shou-Cheng Zhang, and Shanhui Fan, Three-dimensional chiral lattice fermion in Floquet systems, *Phys. Rev. Lett.* **121**, 196401 (2018).
- [40] We set the branch cut of the logarithm along the negative real axis, so  $\ln e^{ika}$  is a sawtooth that jumps at  $ka = \pi + 2n\pi$ .
- [41] G. D. Mahan, *Many-Particle Physics* (Springer, New York, 2000).
- [42] A. Altland and B. Simons, *Condensed Matter Field Theory* (Cambridge University Press, Cambridge, England, 2023).
- [43] The continuum limit  $C_\sigma(k) = -\frac{1}{2} \text{sign}(\sigma k)$  differs from the zero-temperature Fermi function  $\theta(-\sigma k)$  by a 1/2 offset. This offset corresponds to a delta function  $\delta(x - x')$  contribution to the propagator (9), which is lost in the discretization.
- [44] J. Ferrer, J. González, and M.-A. Martín-Delgado, Bosonization on a lattice: The emergence of the higher harmonics, *Phys. Rev. B* **51**, 4807 (1995).
- [45] See Supplemental Material at <http://link.aps.org/supplemental/10.1103/PhysRevLett.133.116501> in which we derive the Euclidean action in the tangent discretization, give details of the quantum Monte Carlo calculation, in particular the check that no sign problem appears, and provide the finite-size corrections to the power law decay of the correlators, following from the bosonization theory [26].
- [46] C. W. J. Beenakker, Topologically protected Casimir effect for lattice fermions, *Phys. Rev. Res.* **6**, 023058 (2024).
- [47] J. Haegeman, L. Lootens, Q. Mortier, A. Stottmeister, A. Ueda, and F. Verstraete, Interacting chiral fermions on the lattice with matrix product operator norms, [arXiv: 2405.10285](https://arxiv.org/abs/2405.10285).
- [48] <https://zenodo.org/doi/10.5281/zenodo.10566063>